Available online at www.sciencedirect.com

SciVerse ScienceDirect

Ceramics International 39 (2013) 3453–3457

CERAMICS INTERNATIONAL

www.elsevier.com/locate/ceramint

Short communication

Thermolysis studies on magnesium zinc bis(citrato)ferrate pentahydrate precursor for synthesis of ferrite nanoparticles

Manpreet Kaur[a,*], B.S. Randhawa[b], Jashanpreet Singh[a,b], Divya Utreja[a]

[a]*Department of Chemistry, Punjab Agricultural University, Ludhiana 141004, India*
[b]*Department of Chemistry, Guru Nanak Dev University, Amritsar 143005, India*

Received 13 July 2012; received in revised form 17 September 2012; accepted 1 October 2012
Available online 17 October 2012

Abstract

Thermolysis of magnesium zinc bis(citrato) ferrate pentahydrate, $MgZn_2[Fe(C_6H_5O_7)_2]_25H_2O$, has been investigated from ambient to 600 °C employing various physico-chemical techniques *viz*. TG–DTG–DSC, IR, XRD and Mössbauer spectroscopy for the characterization of intermediates and final thermolysis products. Dehydration of the precursor completes at 140 °C followed by abrupt exothermic decomposition to yield α-Fe_2O_3, ZnO and MgO as intermediate oxide phases. Finally solid state reaction between oxides results in the formation of spinel ferrite $Mg_{0.3}Zn_{0.7}Fe_2O_4$ as the final thermolysis product at a temperature (350 °C) much lower than for the ammonium substituted citrate precursor (540 °C) and conventional ceramic method (1350 °C). Monodispersed and nanosized nature of ferrite with average particle diameter of 35 nm is confirmed by transmission electron microscopy (TEM). The Mössbauer spectrum of the final thermolysis product displays a doublet owing to the presence of superparamagnetism (SPM) at room temperature. SPM in multi-domain particles is attributed to weakening of A–B exchange interactions, resulting in lowering of anisotropic energy which facilitates onset of SPM at room temperature. Thermolysis pattern has been compared with pure magnesium ferricitrate and ammonium substituted ferricitrate.

Keywords: D. Ferrite; Precursor; Thermolysis; Nanoparticle

1. Introduction

Ferrites are gauged as better magnetic materials than pure metals owing to their reasonable cost, high resistivity, remarkable magnetic properties, easiness of preparation and greater mechanical strength. Spinel ferrites have received immense interest in modern era due to their high permeability in the radio-frequency region [1]. They are extensively used in microwave devices, magnetic drug delivery, ferrofluids and ferroseals [2–8]. AB_2O_4 is a general formula for spinels where tetrahedral (T_d) A sites and octahedral (O_h) B sites are occupied by metal cations. Magnetic properties of ferrites can be suitably modified by varying composition of cations [9]. Zinc and cadmium are non-magnetic ions and preferably occupy T_d sites in the spinel lattice. Occupation of T_d sites by these ions has significant effect on the magnetic behavior and diffusivity of spinels. In comparison to manganese zinc ferrite zinc doped magnesium ferrite is more suited for electronic devices due to better resistivity [10]. Superparamagnetism (SPM) is an interesting phenomenon displayed by ultra-fine ferrite nanoparticles owing to transition from multi-domain to single domain magnetic alignment. In magnesium zinc ferrite, high substitution of zinc can cause SPM at room temperature in even multi-domain particles. This attractive feature makes it a potential candidate to study SPM at room temperature. The conventional ceramic method employed for synthesis of ferrites has two major disadvantages *viz*. high sintering temperature (> 1000 °C) required to overcome reactant barrier and particle coarsening. Milling of starting material introduces lattice defects and strains in the ferrites. Yahya et al. fabricated $Mg_{(1-x)}Zn_xFe_2O_4$ (x=0.2–0.5) by the ceramic route but the sintering temperature requirement was quite high (1350 °C) [11]. For the last few decades, there is surge of

*Corresponding author. Tel.: +91 8146200711.
E-mail address: manpreetchem@pau.edu (M. Kaur).

0272-8842/$ - see front matter © 2012 Elsevier Ltd and Techna Group S.r.l. All rights reserved.
http://dx.doi.org/10.1016/j.ceramint.2012.10.007

interest in synthesizing ferrite nanoparticles by soft chemical methods such as precursor and combustion routes. The precursor method involves atomic scale mixing of metal cations in the precursor moiety which decomposes exothermically, thus lowering the external temperature required for ferrite formation. Evolution of gaseous products dissipates heat and prevents sintering of the final product. Several workers prepared pure and cadmium doped ferrite nanoparticles with well developed spinel phases employing maleate/malonate/citrate precursors and combustion methods [12–19]. Mg–Zn ferrites were synthesized by citrate precursor using the monomer unit $(NH_4)_4\{M[Fe(C_6H_5O_7)]\}$ where M = Mg/Zn and ferrite crystallization was observed at 540 °C [19]. The present investigation is planned to elucidate the synthesis of zinc doped magnesium ferrite via magnesium zinc ferricitrate precursor route. The results are compared with pure magnesium bis(citrate)ferrate decahydrate and ammonium substituted citrate precursor.

2. Experimental procedure

Zinc doped magnesium ferrite was synthesized via citrate precursor route using AR grade chemicals *viz*. magnesium nitrate, ferric nitrate, ferric citrate and citric acid. Double distilled water was used as solvent.

2.1. Preparation of the precursor

Magnesium zinc bis(citrato)ferrate pentahydrate precursor $MgZn_2[Fe(C_6H_5O_7)_2]_2 \cdot 5H_2O$ was synthesized by mixing stoichiometric quantities of aqueous solution of citric acid, ferric citrate, magnesium nitrate and zinc nitrate. The reaction mixture was refluxed at 100 °C for 8 h followed by concentration on water bath. The fluffy concentrated precursor was kept in an oven at 60 °C for 2 h. The resultant precursor powder was washed with ethanol, dried again and stored in a vacuum desiccator. Identity of the precursor was established by elemental analysis: [C% = 25.93(observed), 25.87 (calculated); H% = 2.78(observed), 2.70(calculated); Fe% = 10.35 (observed), 10.32(calculated); Zn% = 11.86(observed), 11.76 (calculated); Mg% = 2.23(observed), 2.16(calculated)].

2.2. Characterization

IR spectrum of the complex and final thermolysis product was recorded on a pye-unicam SP3-300 IR spectrophotometer in the range of 4000–200 cm^{-1} in the KBr matrix. Simultaneous TG–DTG–DSC analysis was carried with a Pyris Diamond Model (Perkin Elmer) at a heating rate of 10 °C min^{-1}. XRD powder patterns were noted with a Panalytical Expert Prompt 2007 instrument using nickel filtered Cu-$K\alpha$ radiation. Scanning electron micrographs (SEM) were visualized with a Hitachi-S-3400N scanning electron microscope at 15.0–20 kV acceleration voltages in SE mode. Sputtering was performed by an E-1010 ion sputter coater to obtain a gold layer of 10–20 nm thickness. Transmission electron micrographs (TEM) of end products were observed with a model Morgagni 268 D HR TEM using water as a dispersion medium. For TEM processing the drop method was employed using carbon coated 200 mesh size copper grids and subsequently the grid was air dried for TEM analysis. A Mössbauer spectrometer (Model MRG 500 Wissel Germany) employing Co^{57} (Rh) as a source was used to record Mössbauer spectra. Mössbauer parameters *viz*. isomer shift (δ) and quadruple splitting (Δ) were determined, and isomer shift values were estimated with respect to a pure iron absorber.

2.3. Calcined powders

For the identification of intermediates and final thermolysis product, the precursor complex was isothermally calcined in a silica crucible in a muffle furnace at different temperatures and time intervals.

3. Results and discussion

3.1. FT-IR studies

IR spectrum (Fig. 1a) of magnesium zinc bis(citrato)-ferrate(III)pentahydrate precursor exhibited a broad band centered around 3450 cm^{-1} due to overlapping of υ(O–H) of citrate group and lattice water. A small shoulder at 3960 cm^{-1} is assigned to υ(O–H) of citrate ligand. A strong band at 1622 cm^{-1} is due to υ_{assym} (C=O) while the band due to υ_{sym} lies in the range 1215–1285 cm^{-1}. Small and distinct bands in the region 1000–1100 cm^{-1} are assigned to υ(C–O), υ(C–C) and (O–H) bending modes. The bands at 560–400 cm^{-1} are assigned to υ(Fe–O) of carboxylate bonding [20]. IR spectrum of the final thermolysis product (Fig. 1b) displayed two absorption bands characteristic of the spinel ferrites at 575 cm^{-1} and 460 cm^{-1}. The higher frequency band was due to stretching vibration of tetrahedral metal oxygen bond and the

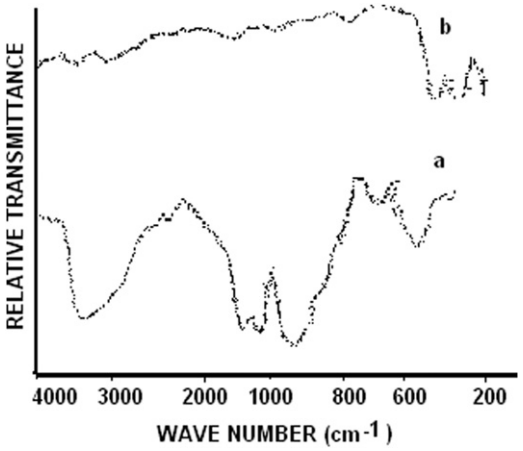

Fig. 1. FT-IR spectrum of (a) precursor and (b) final thermolysis product.

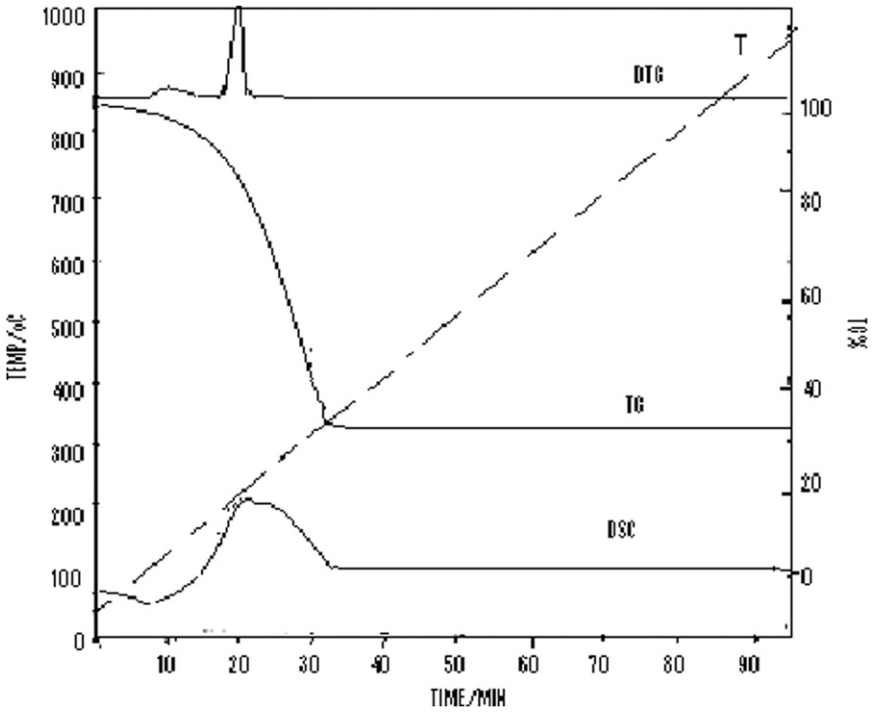

Fig. 2. Simultaneous TG–DTG–DSC thermo gram of the precursor.

lower frequency band was due to octahedral metal oxygen bond.

3.2. Simultaneous thermal analysis and XRD studies

Simultaneous TG–DTG–DSC analysis of the precursor (Fig. 2) reveals that dehydration of the precursor is followed by abrupt exothermic decomposition. Dehydration is completed at 140 °C with mass loss of 7.8% (calculated loss = 8.1%). DTG and DSC (endo $\Delta H = 233.3$ kJ/mole) demonstrated weak signals centered at 100 °C depicting slow rate of dehydration. The unstable anhydrous complex displayed abrupt mass loss upto 67.2% (calculated loss = 67.4%) at 260 °C. The mass loss indicates formation of α-Fe_2O_3, MgO and ZnO. XRD powder pattern (Fig. 3) of the residue calcined at 260 °C for 15 min confirms the formation of α-Fe_2O_3, MgO and ZnO phases [21–23]. DSC shows strong exotherm ($\Delta H = -2683$ kJ/mol) at 190 °C accompanied by DTG peak at 185 °C. Randhawa and Kaur also reported that magnesium bis(citrate)ferrate decahydrate precursor decomposed slowly during the synthesis of $MgFe_2O_4$ with the formation of magnesium acetone dicarboxylate as an intermediate at 150 °C [14]. Likewise, Yang and Yen have also observed Fe(II) intermediate phase in the synthesis of zinc ferrite by the tartarate precursor route [18]. Oxycarbonate with formula $Mg_{2.39}ZnFe_{6.9}(CO_3)_3O_5$ was detected during thermolysis of ammonium magnesium zinc ferricitrate precursor [19]. In the present study, intermediates were not detected. Doping with zinc seems to be related to the instability of anhydrous complex and pyrolysis is

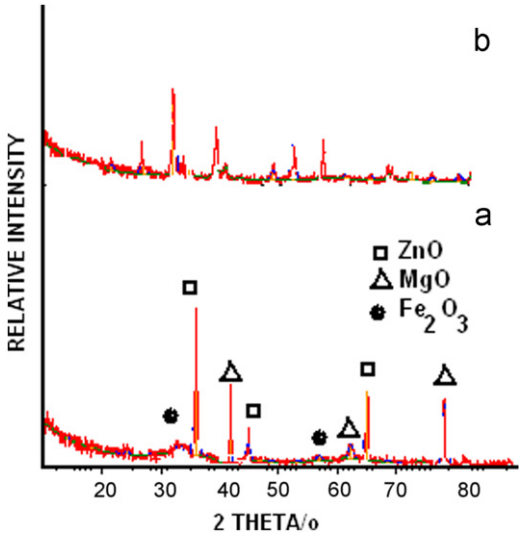

Fig. 3. (a) XRD power pattern of the residue obtained by calcining the parent complex at 200 °C for 15 min and (b) XRD power pattern of the final thermolysis residue.

autocatalysed in the presence of ZnO phase along with α-Fe_2O_3 and MgO. On continuous heating, no further weight loss was evident in TG curve above 315 °C (Fig. 2) and DSC curve displays exothermic region extending up to 350 °C which confirms exothermic solid state reaction between oxides that results in the formation of zinc doped ferrite $Mg_{0.3}Zn_{0.7}Fe_2O_4$ as the final product. Crystallization of ferrite phase from ammonium substituted ferricitrate was noted at higher temperature (540 °C) due to the formation of oxycarbonate intermediate and heat evolved

is used up during cleavage of carbonate whereas direct pyrolysis in the present study lowers the temperature of ferrite formation. As expected, temperature of ferrite formation is much lower than that of the conventional ceramic method (1350 °C) [10]. Moreover, this method does not suffer any drawback of incomplete precipitation as observed in the co-precipitation method. Final thermolysis residue was obtained by calcining the precursor at 350 °C for 3 h and was treated with dilute nitric acid followed by distilled water to remove traces of MgO and ZnO. X-ray diffraction pattern (Fig. 2b) of the final product confirms the formation of spinel ferrite with toichiometry $Mg_{0.3}Zn_{0.7}Fe_2O_4$ [24]. Comparison with the XRD pattern of intermediate clearly indicates transformation of α-Fe_2O_3 into ferrite phase.

3.3. Mossbauer studies

Mössbauer spectrum of the precursor (Fig. 4a) exhibits a doublet with isomer shift and quadruples splitting values of 0.25 and 0.64 mm s^{-1}. These parameters confirm high spin nature of Fe(III) complex in octahedral geometry [25]. Mössbauer parameter values of precursor are in accordance with the findings for ammonium substituted citrate and magnesium bis(citrate)ferrate decahydrate [14,18]. The final thermolysis product (Fig. 4b) displayed superparamagnetic relaxation at room temperature attributed to the fact that Zn^{2+} ions are nonmagnetic and prefer T_d sites owing to their larger ionic radii. Their high concentration results in weakening of A–B exchange interactions. Weakening of coupling lower anisotropic energy and helps in the onset of SPM at room temperature. Mg–Zn ferrites synthesized with the urea–metal nitrate combustion route also displayed decrease in hyperfine field (HF) with increase in Zn^{2+} ion concentration and was attributed to

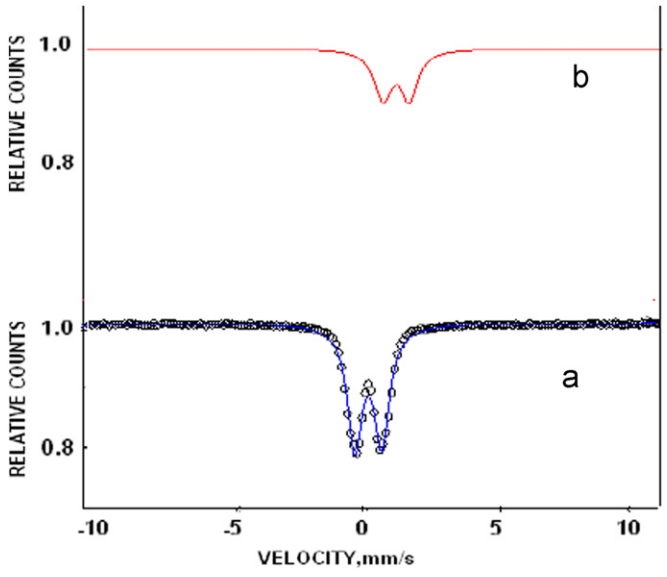

Fig. 4. Mössbauer spectrum of the (a) precursor and (b) final thermolysis product at 300 K.

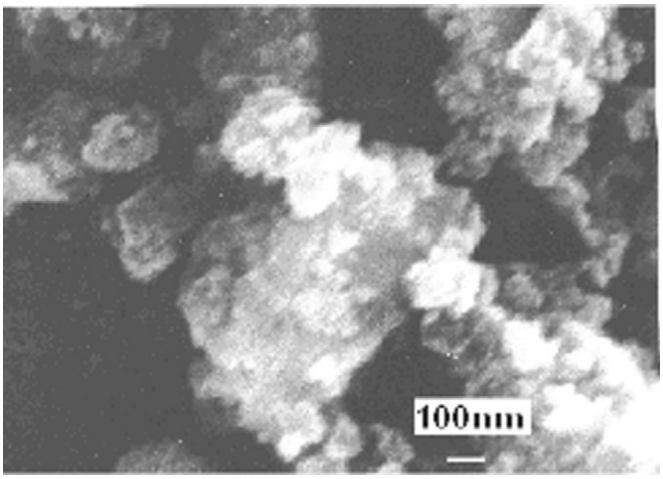

Fig. 5. SEM picture of the final thermolysis product.

the increased possibility of Fe^{3+} ions to locate Zn^{2+} ion as the nearest neighbor [26]. Superparamagnetism was also reported at higher zinc concentration in $Zn_xMn_{1-x}Fe_2O_4$ for $0.5 \leq x \geq 1.0$ [27].

3.4. Microstructural studies

Surface morphology of the final thermolysis product presented in Fig. 5 indicated that magnetic particles agglomerated in powder form and small particles are visible with average diameter of 40 nm, whereas the TEM micrograph of final thermolysis product (Fig. 6) confirms the morphology of nanoparticles and further reveals the formation of ultrafine and well dispersed ferrite nanoparticles with an average particle diameter of 35 nm. Ferrite nanoparticles thus prepared are not a single domain; hence SPM in bigger size particles is solely due to stoichiometry of the final thermolysis product.

On the basis of various physico-chemical studies, the following mechanism for aerial thermolysis of magnesium zinc ferricitrate is proposed:

$$MgZn_2\left[Fe(C_6H_5O_7)_2\right]_2 5H_2O \xrightarrow{140\,^{\circ}C} MgZn_2\left[Fe(C_6H_5O_7)_2\right]_2 + 5H_2O$$

$$MgZn_2\left[Fe(C_6H_5O_7)_2\right]_2 \xrightarrow{260\,^{\circ}C} \alpha - Fe_2O_3 + MgO + 2ZnO$$

$$\alpha - Fe_2O_3 + MgO + 2ZnO \xrightarrow{350\,^{\circ}C} Mg_{0.3}Zn_{0.7}Fe_2O_4 + 0.7MgO + 1.3ZnO$$

4. Conclusion

The citrate precursor approach has been employed to synthesize magnesium–zinc ferrite nanoparticles. Nanophase ferrites with desired stoichiometry were conveniently synthesized by the thermolysis of magnesium zinc ferricitrate precursor. Temperature of ferrite formation is much lower than that of ammonium magnesium zinc ferricitrate complex due to thermolysis of precursor directly into oxide

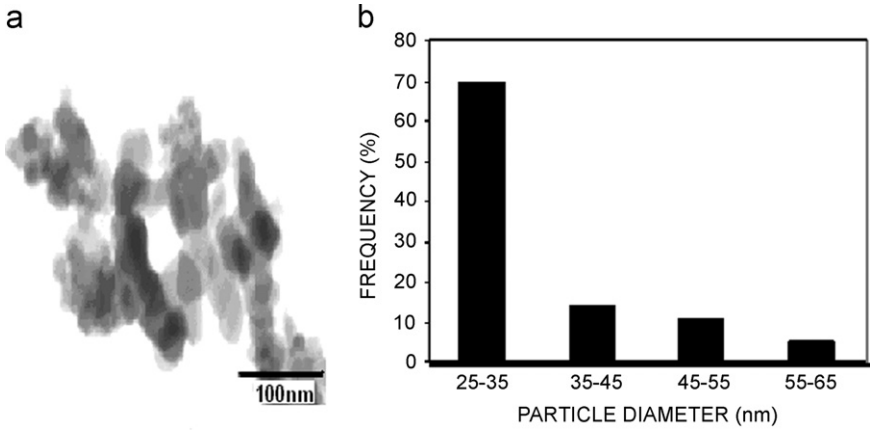

Fig. 6. (a) TEM micrograph of the final thermolysis product and (b) histogram showing particle size distribution.

phase. Mössbauer spectrum of the final thermolysis product displayed superparamagnetic relaxation effect at room temperature for the particles with an average diameter of 35 nm. Exothermic decomposition of precursor liberates enormous heat (clearly evident from ΔH values) to facilitate the solid state reaction between intermediate oxide phases, thus helps in the formation of zinc doped ferrite as the final thermolysis product and ultimately reduces the external required temperature for ferrite formation. Furthermore, gaseous products dissipate heat evolved and prevent sintering of the final thermolysis product.

References

[1] Pe Zbigniew, D. Zich, Microstructural properties of magnesium zinc ferrites as a result of sintering temperature, Journal of the European Ceramic Society 24 (2004) 1053–1056.
[2] F.C.C. Oliveira, L.M. Rossi, R.F. Jardim, J.C. Rubim, Magnetic fluids based on γ-Fe_2O_3 and $CoFe_2O_4$, Journal of Physical Chemistry C 113 (2009) 8566–8572.
[3] F.C. Morals, Photoacoustic spectroscopy as key technique in investigation of nanosized magnetic particles for drug delivery systems, Journal of Alloys and Compounds 483 (2008) 544–548.
[4] J.D. Adams, L.E. David, G.F. Dionne, E.F. Schlemann, S. Stizer, Ferrite devices and materials, IEEE Transactions on Microwave Theory 50 (2002) 721–737.
[5] M.P. Horwath, Microwave applications of soft ferrites, Journal of Magnetism and Magnetic Materials 215 (2000) 171–183.
[6] K. Raj, R. Maskowittz, R. Caseiari, Advances in ferrofluid technology, Journal of Magnetism and Magnetic Materials 149 (1995) 174–180.
[7] F.C.C Oliveira, L.M. Rossi, R.F. Jardim, J.C. Rubim, Magnetic fluids based on γ-Fe_2O_3 and $CoFe_2O_4$, Journal of Physical Chemistry C 113 (2009) 8566–8572.
[8] J. Philip, P.D. Shima, B. Raj, Nanofluid with tunable thermal properties, Applied Physics Letters 92 (2007) 1–3.
[9] B. Viswanathan, V.R.K. Murthy, in: Ferrite Materials, Narosa Publishers, New Delhi, 1990, p. 11.
[10] B. Skolyszewska, Preparation and magnetic properties of Mg–Zn and Mn–Zn ferrites, Physica C 387 (2003) 290–294.
[11] N. Yahya, M.N. Arpin, A.A. Aziz, H. Daud, H.M Zaid., L.K. Pal, N. Mauf, Synthesis and characterization of magnesium zinc ferrite as electromagnetic source, American Journal of Engineering and Applied Sciences 1 (2008) 53.
[12] B.S. Randhawa, K.J. Sweety, M. Kaur, J.M. Greneche, Synthesis of ferrites, Journal of Thermal Analysis and Calorimetry 75 (2004) 101–111.
[13] B.S. Randhawa, H.S. Dosanjh, M. Kaur, Preparation of spinel ferrites by citrate precursor route—a comparative study, Ceramics International 35 (2009) 1045–1049.
[14] B.S. Randhawa, M. Kaur, Preparation of magnesium and calcium ferrites from the thermolysis of $M_3[Fe(cit)_2]_2 \cdot xH_2O$ precursors, Journal of Radioanalytical and Nuclear Chemistry 261 (2004) 569–576.
[15] B.S. Randhawa, M. Gupta, M. Kaur, Synthesis of cobalt ferrite from thermolysis of cobalt tris (malonato) ferrate(III) trihydrate precursor, Ceramics International 35 (2009) 3521–3524.
[16] B.S. Randhawa, M. Kaur, Application of Mossbauer spectroscopy to the thermal decomposition of strontium and barium bis(citrato) ferrates (III), Hyperfine Interactions 188 (2009) 95–101.
[17] M. Kaur, S. Rana, P.S. Tarsikka, Comparative analysis of cadmium doped magnesium ferrite $Mg_{(1-x)}Cd_xFe_2O_4$ (x=0.0, 0.2, 0.4, 0.6) nanoparticles, Ceramics International 35 (2012) 3521–3524.
[18] J.M. Yang, F.S Yen, Evolution of intermediate phase in the synthesis of zinc ferrite nanopowders prepared by the tartarate precursor method, Journal of Alloys and Compounds 450 (2009) 387–394.
[19] V.D.K. Zhetcheva, Characterization of citrate precursor used for synthesis of nanosized Mg–Zn ferrite, Central European Journal of Chemistry 7 (2009) 415–422.
[20] K. Nakamoto, in: Infrared Spectra of Inorganic and Coordination Compounds, 2nd ed., Wiley Interscience, New York, 1970.
[21] ZnO; ASTM Data Card No. 5-0664.
[22] Fe_2O_3; ASTM Data Card No. 13-534.
[23] MgO; ASTM Data Card No. 4–0829.
[24] JCPDS Card No. 00-008-0234.
[25] A. Vertes, L. Korecz, K. Burger, in: Mössbauer Spectroscopy, Elsevier, New York, 1979, p. 47.
[26] R.G. Kulkarni, H.H. Joshi, Magnetic properties of Mg–Zn ferrite system by Mossbauer spectroscopy, Solid State Communications 53 (1985) 1005–1008.
[27] D. Varshney, K. Verma, A. Kumar, Structural and vibrational properties of $Zn_xMn_{1-x}Fe_2O_4$ mixed ferrites (x=0.0, 0.25, 0.50, 0.75, 1.0), Materials Chemistry and Physics 131 (2011) 413–419.